

PACS numbers: 42.55.Vc; 52.38.Ph; 53.50.Jm
DOI: 10.1070/QE2012v042n11ABEH014747

X-ray lasing on the 4d–4p transitions of Ni-like molybdenum ions

A.V. Andriyash, D.A. Vikhlyaev, D.S. Gavrilov, S.A. Gorokhov, D.A. Dmitrov, A.L. Zapysov, A.G. Kakshin, I.A. Kapustin, E.A. Loboda, V.A. Lykov, V.Yu. Politov, A.V. Potapov, V.A. Pronin, G.N. Rykovanov, V.N. Sukhanov, A.A. Ugodenko, O.V. Chefonov

Abstract. **We outline the results of experiments in the generation of X-ray laser radiation on the 4d–4p Ni-like ion transitions at a wavelength λ = 189 Å under sequential irradiation of plane targets by two laser pulses focused to a line. These experiments were executed on the Sokol-p picosecond laser facility. The average energy of a 4-ps long ultrashort pump pulse was equal to 6.5 J, the energy of a 0.44-ns long prepulse was equal to 2.7 J, and the time delay between them was equal to 1.5 ns. The effective gain for short target lengths was equal to ~24 cm^{-1}. In the travelling pump wave regime, which was realised using a ladder mirror, we obtained an 8-fold increase in output X-ray laser energy in comparison with the output energy obtained in the ordinary target irradiation regime.**

Keywords: *X-ray laser, laser radiation, Ni-like molybdenum ions.*

1. Introduction

Since the first demonstration of the amplification of soft X-ray spontaneous emission [1, 2], the development and investigations of X-ray lasers (XRLs) are being carried out intensively, both theoretically and experimentally, in many laboratories in the world. A major impetus for the progress of laboratory XRLs was lent by a paper [3], which was published by P.N. Lebedev Physics Institute scientists, who provided a theoretical substantiation for the scheme of transient collisional excitation of the active medium using an ultrashort pulse (USP) of laser radiation. The main virtue of this scheme consists in the absence of limitations on the electron density of the active medium and the possibility of obtaining a high gain. For the first time an XRL with transient collisional pumping was experimentally demonstrated in Ref. [4], in which a gain $g \approx 20$ cm^{-1} was realised under sequential target irradiation by nanosecond and picosecond pulses with moderate energies (4 and 7 J, respectively).

A.V. Andriyash, D.A. Vikhlyaev, D.S. Gavrilov, S.A. Gorokhov, D.A. Dmitrov, A.L. Zapysov, A.G. Kakshin, I.A. Kapustin, E.A. Loboda, V.A. Lykov, V.Yu. Politov, A.V. Potapov, V.A. Pronin, G.N. Rykovanov, V.N. Sukhanov, A.A. Ugodenko, O.V. Chefonov E.I. Zababakhin All-Russian Scientific-Research Institute of Technical Physics, Russian Federal Nuclear Centre, ul. Vasil'eva 13, 456770 Snezhinsk, Chelyabinsk region, Russia; e-mail: dep5@vniitf.ru

Received 5 October 2011; revision received 1 September 2012
Kvantovaya Elektronika **42** (11) 985–988 (2012)
Translated by E.N. Ragozin

The main disadvantage of the transient collisional pumping scheme is the effect of radiation delay. To eliminate this effect, in Ref. [5] advantage was taken of a travelling pump wave produced with the help of a ladder mirror. For a total laser pump energy of ~7 J, it was possible to achieve a saturation regime for the generation of X-ray laser radiation (XRLR) at a wavelength λ = 147 Å using Ni-like Pd ions. The output energy of XRL radiation beam was equal to 12 μJ.

The requirements imposed on the laser energy are significantly relaxed when the target is irradiated using a grazing incidence pump (GRIP) scheme. In this case, the USP is focused onto the target at an incidence angle of 70°–80° using a long-focus lens. Automatically realised in this case is the velocity of pump radiation propagation along the target surface close to the velocity of light (a travelling wave); furthermore, the pump radiation is more efficiently absorbed in the active medium of the XRL [6]. The GRIP scheme was employed to obtain X-ray lasing in a repetitively pulsed regime (~10 Hz) using table-top laser facilities with pulse energies of ~1 J [7–9]. This was a major advance, which enabled employing XRLs in areas of practical importance like X-ray microscopy and lithography, and investigations of the properties of the surface layers of solids. The energy of one XRL pulse in the experiments involving the GRIP scheme amounted to 0.01–1 μJ. Operation in the repetitively pulsed regime enables accumulating over an acceptable irradiation time (~1 h) a significant dose (up to 50 mJ) in the sample under irradiation [8].

The Sokol-p facility is actively used to carry out experiments to investigate the properties of laser plasmas produced in the interaction of laser USPs with solid targets at intensities up to 3×10^{19} W cm^{-2} [10]. The application of an XRL opens up fresh possibilities for the diagnostics of the state of these plasmas. The short XRL pulse duration in comparison with characteristic hydrodymanic motion times permits obtaining virtually 'instantaneous' snapshots of the electron density (N_e) distribution [11]. The short (λ = 189 Å) XRL wavelength makes it possible to probe plasma domains with N_e as high as 10^{24} cm^{-3}. The objective of the experiments outlined in the present work was to make an XRL constituting a high-power backlighting source for the investigation of expansion dynamics of a dense plasma. These experiments continue the series of experiments to realise an XRL with transient collisional pumping on the Sokol-p laser facility [12]. Going over from Ne-like ions to Ni-like ions permitted us to shorten the XRL wavelength by a factor of 1.7 with retention of the pump energy, while the use of a travelling pump wave enabled obtaining a saturation XRL operation regime with an output energy sufficient for probing applications.

2. Experimental conditions

The experimental setup is schematically shown in Fig. 1. For a target (*5*) use was made of plane polished plates of molybdenum ranging from 2 to 8 mm in length. The target was sequentially irradiated by two laser pulses with a radiation wavelength $\lambda = 1.06$ μm: the 400-ps-long prepulse and the main 4-ps-long pump pulse. The average on-target energy of the USP pump was equal to 6.5 J, the prepulse energy was equal to 2.7 J, and the delay between them amounted to 1.5 ns. The optical system that formed the temporal shape of laser radiation was described at length in Ref. [12]. The beam was injected into the vacuum target chamber via a lithium fluoride entrance window (*3*). The laser radiation was focused to a narrow focal line using an optical system comprising a meniscus (*2*) and an elliptic paraboloid (*4*). In the preliminary series of experiments we optimised the conditions of target irradiation: the focal line width was varied from 30 to 120 μm. The maximum energy of lasing was observed for a focal line width of 80–90 μm. This corresponds to a laser radiation intensity of $\sim 10^{12}$ W cm^{-2} for the prepulse and to 2.5×10^{14} W cm^{-2} for the main USP. The spatial characteristics of the laser beam and of the optical system formed an irradiation intensity distribution which was uniform to within ±20% along the focal line.

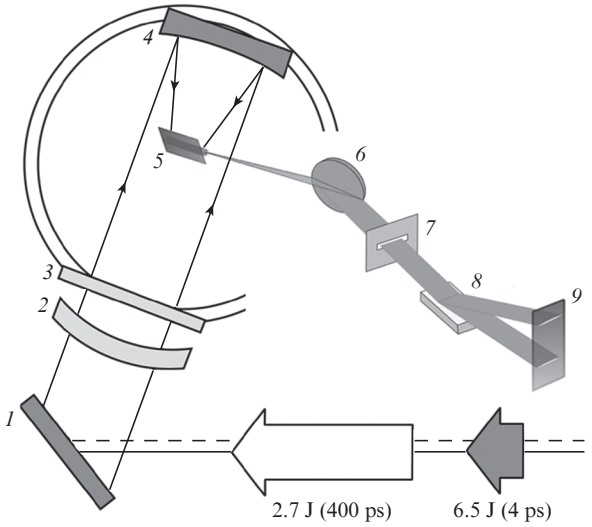

Figure 1. Schematic of X-ray lasing experiments: (*1*) mirror; (*2*) meniscus; (*3*) window of the target chamber; (*4*) elliptic paraboloid; (*5*) target; (*6*) focusing spherical mirror; (*7*) spectral slit; (*8*) diffraction grating; (*9*) CCD camera.

To record the radiation spectrum in the direction of the focal line of the pump radiation, use was made of a spectrograph–divergence analyser, which comprised two X-ray optical elements: a grazing incidence focusing mirror (*6*) and a plane diffraction grating (*8*). The grating efficiency in the first diffraction order for a wavelength $\lambda = 189$ Å was measured at 3.2% using an RKK-1-100 stationary X-ray facility [13]. The mirror was oriented perpendicular to the diffraction grating and collected the rays in the plane perpendicular to the target plane. The target centre was almost exactly in the meridional focal plane of the mirror, which thereby forms a nearly parallel ray bundle and permits analysing the XRLR divergence in the plane perpendicular to the target plane. The target radiation reflected from the mirror passed through a spectral slit (*7*) and, on reflection from the diffraction grating (*8*), was recorded with a CCD camera (9).

The dynamic range of the CCD camera employed to record the spectrum is determined, on the one hand, by the capacity of an array pixel and, on the other, by the background level. In real experiments the dynamic range amounted to $\sim 10^3$ owing to significant background illumination due to continuous plasma radiation diffracted by the spectrograph's grating and the parasitic scattered radiation penetrating into the spectrograph through the slit. We employed replaceable slits to broaden the dynamic range. For a short target lengths and the consequential low lasing energies, use was made of a 120-μm-wide slit, which corresponded to the optimal spectral resolution $\lambda/\Delta\lambda \sim 140$. For higher XRLR energies the slit width was decreased to 14 μm. The decrease in slit dimensions in combination diffraction image broadening results in a 24-fold lowering of the photon flux at the CCD array.

In the present work, to increase the absolute XRLR yield for a large target length we implemented the regime of travelling pump wave similar to that described in Ref. [5]. For this purpose, a ladder mirror consisting of six elements (Fig. 2) was mounted in the optical target irradiation system in place of the plane mirror (*1*). Each element of the ladder mirror is a rectangular plate with a reflection coefficient $R =$

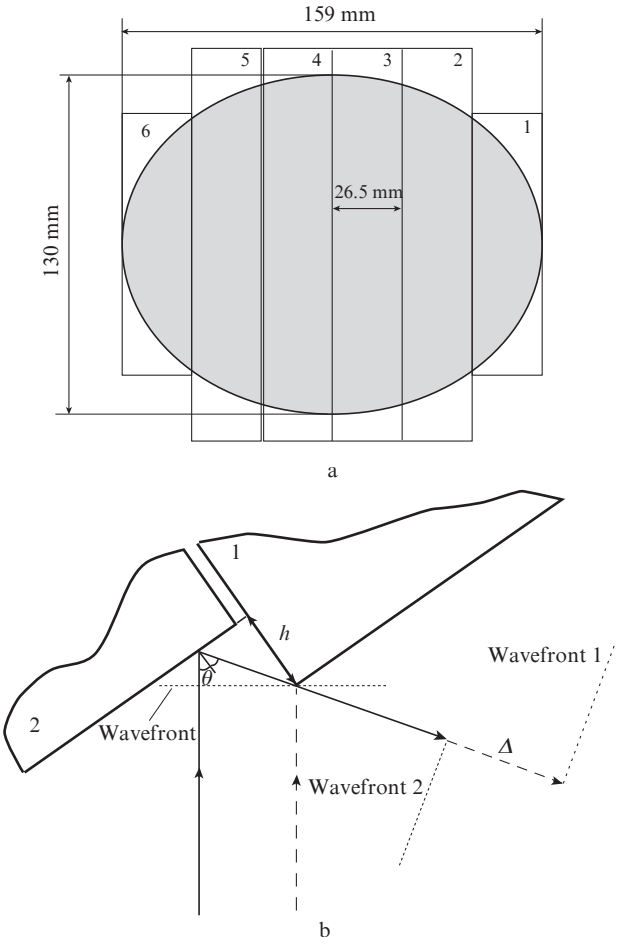

Figure 2. Ladder mirror: front view (the filling of the mirror aperture by the heating laser pulse) (a) and top view (formation of the time delay in the irradiation of neighbouring target elements) (b).

0.98% at $\lambda = 1.054$ μm for an incidence angle $\theta = 35°$. The surfaces of these mirrors are parallel to each other. A specialised alignment device permits adjusting each element independently, both in angle and step height. With the help of the focusing system, each element of the mirror forms a 1.67-mm long segment of the focal line on the target plane. The step height h between the neighbouring plates defines the time delay for the irradiation of the neighbouring elements of the focal line.

3. Experimental results

Figure 3 shows the spectrogram obtained in an experiment with a target of length $l = 8$ mm. The brightest line in the right part of the image corresponds to the first order of reflection from the diffraction grating for the lasing line with $\lambda = 189$ Å; recorded in the left part of the image is the lasing line in the second order of reflection.

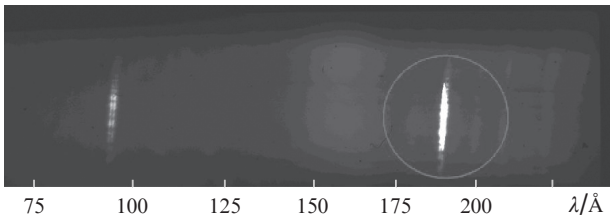

Figure 3. Spectrogram of XRLR with a wavelength $\lambda = 189$ Å for a target length $l = 8$ mm.

Figure 4 shows the experimental dependences of the XRLR yield on the target length. The effective XRLR small-signal gain g estimated from the exponential portion of the curve amounts to 25–30 cm^{-1}. Therefore, for the maximum target length $l = 8$ mm, the gain-length product $gl = 20–24$. The data of our experiments testify that a certain increase in XRLR yield in the travelling pump wave regime is observed even for $l = 4–5$ mm. For 8-mm-long targets the travelling wave regime provides an approximately eight-fold gain in comparison with the ordinary irradiation regime. In this case, the highest XRLR energy was equal to 3.5 μJ.

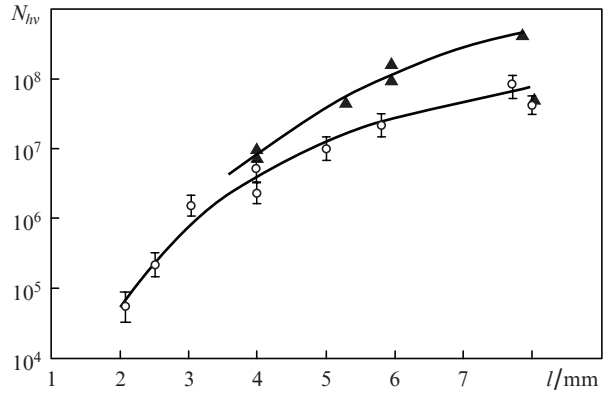

Figure 4. Experimental dependences of the XRLR yield N_{hv} on the target length l obtained in the ordinary target irradiation regime (○) and in the travelling pump wave regime (▲) (N_h is the number of photons integrated over the CCD-captured image of the lasing line).

4. Discussion of results

The large value of the gl product (29–24) obtained in the present work testifies to a close-to-saturation XRL operation regime. At the same time, the output energy in the regime with a travelling pump wave was only one order of magnitude higher than in the regime without it. In the experiments of Ref. [5], which were close to our experiments as regards target irradiation parameters, the use of the travelling pump wave regime enabled an approximately 100-fold increase in XRLR energy and its absolute value was 2.5 times higher than that obtained in the present work. Among the most likely reasons accounting for the difference in the data is the nonuniformity of target irradiation, with the result that the intensity of the heating pulse, and hence the gain, are significantly lower at the edges of the active medium. Therefore, the possibility of improving the output characteristics of the XRLR beam on the Sokol-p facility consists in improving the spatial characteristics of the beam focused to a line. The resultant output laser energy (3.5 μJ) nevertheless permits us to implement on its basis a backlighting source for probing dense regions of laser plasmas.

5. Conclusions

Experiments to generate XRLR at a wavelength $\lambda = 189$ Å on the 4d–4p transitions of Ni-like molybdenum ions were performed on the Sokol-p picosecond laser facility. These experiments demonstrate the generation of XRLR in the transient collisional pumping scheme under the irradiation of targets by two laser pulses of nano- and picosecond duration, which were focused to an 80–90-μm-wide line up to 8 mm in length. The respective intensities of laser irradiation for the prepulse and the main USP were equal to $\sim 10^{12}$ and $\sim 2.5 \times 10^{14}$ W cm^{-2}.

In these experiments we obtained the dependence of the XRLR yield on the target length, which was varied from 2 to 8 mm. A travelling pump wave regime was realised with the use of a ladder mirror. For the longest target (8 mm), an approximately eight-fold increase in XRLR yield was obtained, the highest XRL beam energy being equal to 3.5 μJ. In the future, we plan to employ the XRL as a backlighting source for probing the dense plasma regions of laser USP-irradiated targets.

References

1. Matthews D.L., Hagelstein P.L., Rosen M.D., et al. *Phys. Rev. Lett*., **54**, 110 (1985).
2. Suckewer S., Skinner C.H., Milchberg H., et al. *Phys. Rev. Lett*., **55**, 1753 (1985).
3. Afanas'ev Yu.V., Shlyaptsev V.N. *Kvantovaya Elektron*., **16**, 2499 (1989) [*Sov. J. Quantum Electron*., **19**, 1606 (1989)].
4. Nickles P.V., Shnurer M., Kalashnikov M.P., et al. *Proc. SPIE Int. Soc. Opt. Eng*., **2520**, 373 (1995).
5. Dunn J., Li Y., Osterheld A.L., et al. *Phys. Rev. Lett.*, **84**, 4834 (2000).
6. Keenan R., Dunn J., Patel P.K., et al. *Phys. Rev. Lett*., **94**, 103901 (2005).
7. Luther B.M., Wang Y., Larotonda M.A., et al. *Opt. Lett*., **30** (2), 165 (2005).
8. Zielbauer B., Zimmer D., Habib J., et al. *Appl. Phys. B,* **100**, 731 (2010).
9. Habib J., Guilbaud O., Zielbauer B., et al. *Opt. Express*, **20** (9), 10128 (2012).

10. Afonin V.I., Vikhlyaev D.A., Gavrilov D.S. et al. *Vopr. Atom. Nauki Tekh., Ser. Termoyad. Sintez*, (1), 63 (2011).
11. Smith R.F., Dunn J., Nilsen J., et al. *Phys. Rev. Lett*., **89**, 065004 (2002).
12. Andriyash A.V., Vikhlyaev D.A., Gavrilov D.S., et al. *Kvantovaya Elektron*., **36**, 511 (2006) [*Quantum Electron.*, **36**, 511 (2006)].
13. Gilev O.N., Vikhlyaev D.A., Eliseev M.V., et al. *Prib. Tekh. Eksp*., (1), 119 (2008).